Surface Electrode Mechanism Associated with Preceding and Follow up Chemical Reactions – Theoretical Analysis in Square-Wave Voltammetry

Pavlinka Kokoskarova, Sonja Risafova, Rubin Gulaboski*

Faculty of Medical Sciences, Goce Delcev University Stip, Macedonia
* Corresponding author's e-mail address: rubin.gulaboski@ugd.edu.mk

Abstract: Surface electrode reaction (E), coupled with reversible preceding and reversible follow up chemical steps (C), or so-called "surface CEC mechanism" is considered theoretically under conditions of square-wave voltammetry. Large set of square-wave voltammograms of considered electrode system are calculated as a function of thermodynamics and kinetics of chemical steps involved in this complex mechanism. The surface CEC mechanism can be simplified to a surface CE, or a surface EC mechanism, if one assumes defined magnitudes of the equilibrium constants of chemical steps involved. Although the influence of the square-wave frequency to the voltammetric patterns is quite complex, a frequency analysis can reveal important aspects to recognize this mechanism. While we present important differences that can distinguish between the effect of the kinetics of both chemical steps, we also give the readers hints on how to design experiments in order to get access to all relevant kinetic constants. Theoretical results elaborated in this work are quite important, since there are important experimental systems, such as redox enzymes and metal-ligand complexes, whose voltammetric behaviour fits to this mechanism.

Keywords: surface electrode mechanism, protein-film voltammetry, CEC mechanism, kinetics chemical reaction, kinetics of electrode reaction.
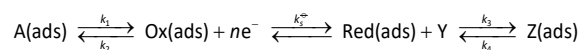
INTRODUCTION

IN the last 30 years, square-wave voltammetry (SWV) emerged as one of the leading electrochemical techniques to monitor relevant mechanistic, kinetics and thermodynamic aspects of important redox systems.[1–8] The measuring performances of the SWV, outlined mainly in the measuring speed and the capability for significant distinction of the Faradaic *vs.* the capacitance currents, make this technique suitable tool for getting access to relevant electrochemical features of important chemical systems[1–4] Electrochemical systems that are associated with chemical equilibria attract significant voltammetric interest, since they are commonly encountered in chemistry, biochemistry and physiology.[1,4,5,9–13] Many of these systems are considered as adequate models that provide insight into relevant physiological functions of pertinent compounds such as the redox enzymes.[5,6,10–13] Principally, for the so-called "surface-active" chemical systems, voltammetry is recognized as very efficient

technique, capable to provide mechanistic, thermodynamic and kinetic information for large set of lipophilic compounds.[1,5,9–11] When it is about electrochemistry of the so-called "lipophilic redox enzymes", the protein-film voltammetry (PFV)[5,6,11–13] is recognized as a very simple, cheap and systematic methodology. This technique is designed to enable access to important physical parameters associated to the chemical behavior of many redox enzymes.[5,6,12,13] The distinctive capabilities of PFV are mainly reflected in the simple experimental set up used in this technique.[12,13] In several recent theoretical works, this technique, under conditions of square-wave voltammetry, has been applied for understanding a large set of complex electrochemical aspects of surface-confined substrates and redox proteins, whose electrode transformation was assumed to be associated with various chemical equilibria.[6,14–21] Electrochemical systems, which comprehend electron transfer step that is coupled with two different chemical reactions, show rather complex behavior under voltammetric conditions.[9,10,14,22] This is because of the

simultaneous interplay of both chemical steps to the electron transfer reaction, but also due to eventual mutual interaction of both chemical steps.[14,22] Although there are important experimental electrochemical systems, in which preceding and follow up chemical reactions are both associated to a given electrode reaction,[5,9,12,13] the voltammetric theories of such mechanisms are rather rare.[2,14,22] In this work, we consider theoretically, under conditions of SWV, a surface electrode reaction that is associated with reversible preceding and reversible follow-up chemical steps. The common electrochemical abbreviation of this mechanism is a "surface CEC mechanism". We present in this work a large set of calculated SW voltammetric patterns, which might help the readers in resolving relevant aspects of this complex mechanism. Importance of the theoretical results evaluated for this mechanism is seen in the redox chemistry of important biomolecules such as quinones and some neurotransmitters,[23] redox enzymes,[12,13] thiols,[24,25] and some lipophilic metal-ligand complexes.[26–30]

Mathematical Model

Surface electrode mechanism, in which the electron exchange step between the working electrode and the redox active substrate is associated with preceding and follow up chemical reaction, is considered theoretically under conditions of square-wave voltammetry. The abbreviation of corresponding electrochemical system is a "surface $C_{rev}EC_{rev}$" mechanism (or simply "surface CEC mechanism"). The term "E" stays to denote the electron transfer step taking place between the working electrode and the redox active substrate, while "C" refers to the chemical reactions involved in this mechanism. In the mathematical model, we assume that all relevant species are firmly adsorbed ("ads") to the surface of the working electrode, while forming a uniform monolayer of adsorbed molecules. We also assume that both chemical reactions involved in this mechanism are of reversible nature. The initial electrochemically active species Ox(ads) are created via dissociation from A(ads) species. The electrochemical step "E" encompasses an electron exchange between the working electrode and the chemically generated redox form Ox(ads), which gives as products reduced form of electrochemically active species-Red(ads). In a final chemical step, the species Red(ads) are involved in a chemically reversible reaction with the substrate Y, while creating Z(ads) species. Z(ads) is a symbol of electrochemically inactive species, emerging as a final product in this complex mechanism. A simplified scheme of the elaborated surface $C_{rev}EC_{rev}$ mechanism is as follows:

$$A(ads) \underset{k_2}{\overset{k_1}{\rightleftarrows}} Ox(ads) + ne^- \underset{}{\overset{k_s^\ominus}{\rightleftarrows}} Red(ads) + Y \underset{k_4}{\overset{k_3}{\rightleftarrows}} Z(ads)$$

For solving of this model, we suppose that only the species "A", and "Y" are present in the electrochemical cell at the point $t = 0$ of the voltammetric experiment. In the second approximation of the mathematical model, it is assumed that there are no interactions between substrates "A" and "Y" of any kind. This holds true also for the species "A" and "Z". In addition, it is supposed that there is absence of any kind of interactions between all species that stay immobilized at the working electrode surface. "Y" is a symbol of the substrate that is present in excess in the voltammetric cell, and exhibits no electrochemical activity in the potential region explored in the voltammetric experiments. "Y" is supposed to react in a selective and chemically reversible fashion with Red(ads) species, while generating the electrochemically inactive species Z(ads). Mathematically, this mechanism can be represented with following sets of equations:

$t = 0; \ \Gamma(A) = \Gamma^*(A) / (1 + K_{eq, \ preceding}); \$ and

$\Gamma(Ox) = K_{eq, \ preceding} \ \Gamma^*(A) / (1 + K_{eq, \ preceding}); \ \Gamma(Red) = 0$ 　(a)

$t > 0; \ \Gamma(A) + \Gamma(Ox) + \Gamma(Red) + \Gamma(Z) = \Gamma^*(A);$ 　(b)

$t > 0; \ K_{eq, \ preceding} = k_1/k_2; \ K_{eq, \ follow-up} = k_3/k_4$ 　(c)

For $t > 0$, the following differential equations (d–f) link the surface concentrations with the current and the kinetics and thermodynamics of preceding and follow-up chemical steps:

$d\Gamma(A) / dt = k_1\Gamma(A) - k_2\Gamma(Ox)$ 　(d)

$d\Gamma(Ox) / dt = -I / (nFS) - k_2\Gamma(Ox) + k_1\Gamma(A)$ 　(e)

$d\Gamma(Red) / dt = I / (nFS) - k_3\Gamma(Y) + k_4\Gamma(Z)$ 　(f)

The electric current, the applied electrical potential difference, the surface concentrations of the electrochemically active species, and the other parameters relevant to electron transfer step are assumed to be interrelated via the Butler-Volmer equation, having the following form:

$(I / nFS) \ = k_s^\ominus exp(-\alpha\Phi) \ [\Gamma(Ox) \ - \ exp(\Phi) \ \Gamma(Red)]$ 　(g)

In the supplementary material of this work, we provide the readers entire working MATHCAD file. It contains all recurrent formulas, and all relevant parameters needed for simulations of theoretical voltammograms of the surface CEC mechanism. We ascribed the positive sign to the forward (reduction) currents (blue color), and negative sign (red color) is ascribed to the backward (oxidation) currents. The resulting net-SWV currents are designated with black color at all voltammograms. In all simulations, the starting potential was set to positive value, and it runs toward negative final potentials in all experiments.

Description of the Relevant Parameters that Affect the Features of Theoretical Square-wave Voltammograms

In the mathematical model, the dimensionless current Ψ of calculated SW voltammograms is defined as $\Psi = I/[(nFSf\Gamma^*)]$. In last definition of Ψ, symbol "I" stays for the electric current, while "n" designates the number of electrons involved in the electron-exchange step between the working electrode and the redox active species. With "S" we assign the active area of the working electrode, while "f" is the frequency of SW pulses. The SW frequency f is defined as $f = 1/(2t_p)$, where t_p is a time-duration of a single SW potential pulse. The symbol "Γ^*" stays for the initial surface concentration of adsorbed A(ads) species, and it equals the total surface concentration of all adsorbed species. The dimensionless potential ϕ is defined as $\phi = nF(E - E^{\ominus}/RT)$, where $E^{\ominus}$ *is the* standard redox potential of Ox/Red couple, while α is the electron transfer coefficient (it was set to $\alpha = 0.5$ in all simulations). T is symbol of the thermodynamic temperature (T was set to 298 K in all calculations), R is the symbol for universal gas constant, and F is the Faraday constant. In addition, the relevant characteristics of calculated SW voltammograms are affected by several dimensionless parameters. The dimensionless electrode kinetic parameter $K_{ET} = ks^{\ominus}/f$ relates the standard rate constant of electron transfer ks_o to the time duration of potential pulses applied in SWV. Furthermore, the relevant attributes of calculated voltammetric patterns are affected by two dimensionless chemical kinetic parameters, $K_{chem-preceding}$, and $K_{chem-follow\ up}$ defined as: $K_{chem-preceding} = \varepsilon/f$, and $K_{chem-follow\ up} = z/f$. In last two equations, $\varepsilon = (k_1 + k_2)$ and $z = (k_3 + k_4)$, are cumulative chemical rate parameters of the preceding and follow up chemical reaction, respectively. $K_{chem-preceding}$ reflects the rate of the preceding chemical step relative to the time-frame of current measurement in SWV. The chemical parameter "z", which appears in the definition of $K_{chem-follow\ up}$, is related to the rate of the overall follow-up chemical reaction, and it is defined as: $z = (k_3 + k_4)/f$. However, since we assume an excess of "Y" substrate in electrochemical cell, the concentration of "Y" will be held constant at the working electrode surface in the course of voltammetric experiment. Therefore, the chemical step in the follow-up reaction is considered to be of pseudo-first order, and the chemical rate parameter of follow up reaction (z) can be also written as: $z = [k_3^{\ominus}c(Y) + k_4]/f$. In the last equation, $c(Y)$ is the molar concentration of substrate "Y" present in excess in voltammetric cell, while $k_3^{\ominus}$ is a real rate constant of the forward step of follow-up chemical reaction. In addition, the features of calculated SW voltammograms are function of two chemical equilibrium constants: one of preceding chemical reaction $K_{eq,\ preceding}$, defined as $K_{eq,preceding} = k_1/k_2$, and one of the follow-up chemical

reaction $K_{eq,\ follow\ up}$, defined as $K_{eq,\ follow\ up} = k_3/k_4$. The magnitudes of both chemical equilibrium constants are linked to the quantities of Ox(ads) and Red(ads) that stay available for electrode transformation. If not otherwise stated, we set in all simulations the SW potential parameters to following magnitudes: frequency $f = 10$ Hz, amplitude $E_{SW} = 50$ mV, and potential step $dE = 4$ mV. More details about the algorithm used are reported in.[1,11] "MATHCAD 14" commercial software was explored for calculating the SW voltammograms reported in this work.

RESULTS AND DISCUSSION

The protocol in which theoretical data are treated for given electrode mechanism depends primarily upon whether the technique explored can provide a direct access to the parameters affecting the relevant features of elaborated mechanism. A conventional way of handling the theoretical data in SW voltammetry commonly considers construction of working curves that allow insight into some aspects of the reaction mechanism. Such working curves also offer protocols to develop methodologies for estimation of relevant physical parameters.[1,4,11] The most common analysis in theoretical voltammetric studies is related to time-dependences (i.e. frequency or scan rate dependence) of the voltammetric responses. However, the time-analysis in voltammetry can often lead to misinterpretation of the obtained data, especially if considered electrode mechanisms are associated with chemical equilibria. This is due to simultaneous effect of frequency (or scan rate) to both-to the kinetic parameter of electron transfer step, and to the rates of chemical reactions of CEC mechanism as well. Since the elaborated surface CEC mechanism is quite complex, a better strategy is to simplify it to its limiting situations. The voltammetric complexity of considered surface CEC mechanism can be initially simplified, by taking into consideration defined magnitudes of both equilibrium constants of chemical reactions: (1) If $K_{eq-follow\ up} < 0.005$ and for $K_{chem-follow\ up} < 0.05$, the entire surface CEC mechanism turns into a surface $C_{rev}E$ mechanism; (2) If the magnitude of $K_{eq,\ preceding} > 10$, then the surface EC_{rev} mechanism comes out as a limiting case of the surface CEC mechanism; (3) In scenario when $K_{eq,\ preceding} \leq 1$, and $K_{eq,\ follow\ up} \leq 1$, one obtains very complex voltammetric patterns. In such cases, the shape and the position of calculated voltammetric outputs is a complex function of the kinetics and thermodynamics of both chemical steps.

(1) If $K_{eq,\ follow\ up} < 0.005$, and for values of $K_{chem-follow\ up} < 0.05$, the voltammetric patterns of a surface CEC mechanism are identical to those of a surface $C_{rev}E$ mechanism (Figure 1.).[1,11,15] In this scenario, the protocols reported in Ref. [15] can be explored to get access to the kinetic and thermodynamic parameters relevant the

electron transfer step, but also the thermodynamic and kinetic parameters related to the preceding chemical reaction, as well.

It is worth to note that if equilibrium constant of the preceding chemical reaction $\log(K_{eq,preceding}) \leq 0$, one observes obvious effects of dimensionless chemical parameter $K_{chem-preceding}$ to the features of calculated SW voltammograms. As expected (see Figure 1.), an initial increase of $K_{chem-preceding}$ from 0.01 to 1, causes significant effects to all current components of calculated SW voltammograms. At $\log(K_{chem-preceding}) \geq 1$, one gets voltammograms as typical of a "simple surface mechanism", whose features get independent on $K_{chem-preceding}$. If $\log(K_{eq,\ preceding}) > 2$, the dimensionless currents get constant value, regardless of the value of dimensionless chemical rate parameter of the preceding step. In such case, there will be a strong shift of the equilibrium of preceding chemical step towards the chemically generated products (Ox(ads)), so the overall mechanism turns to a "simple surface electrode reaction".[1] For a given value of the dimensionless kinetic parameter of electron transfer K_{ET}, roughly in the regions of $-2 < \log(K_{eq,\ preceding}) < 1.5$, one recognizes existence of so-called "kinetic zones" in the curves of $\Psi_{net,p}$ and $E_{net,p}$ *vs.* $\log(K_{chem-preceding})$ (see linear parts of curves in Figure 2.). In the mentioned regions, the kinetic of preceding chemical step influences significantly both the net SW peak potentials $E_{net,p}$, and the net SW peak currents $\Psi_{net,p}$ of simulated voltammograms (see linear parts at Figures 2.A and 2.B). The slopes of the linear parts of the $E_{net,p}$ *vs.* $\log(K_{chem-preceding})$ curves (Figure 2.B) are defined as $2.303 RT/nF \log[K_{eq,preceding}/(1 + K_{eq,\ preceding})]$. This implies that the dependence of $E_{net,p}$ *vs.* $\log(K_{chem-preceding})$ in the "chemical kinetic zones" presented in Figure 2.B, can be explored to determine the value of $K_{eq,\ preceding}$, provided that the parameters of the electron transfer step of electrode reaction are previously determined.[15]

As elaborated in Refs. [1,11], a very specific feature of all surface electrode mechanisms is the parabolic dependence of the $\Psi_{net,p}$ as a function of the dimensionless kinetic parameter related to electron transfer step K_{ET}. This parabolic dependence of $\Psi_{net,p}$ *vs.* K_{ET}, known as "quasireversible maximum", is established as a very simple tool to get access to standard kinetic constant related to the electron transfer rate.[1] In Refs. [1,15], it has been shown that for the surface CE mechanism, this phenomenon is virtually independent on $K_{chem-preceding}$ and $K_{eq,\ preceding}$ (see Figures 3. and 4.). Consequently, the phenomenon of "quasireversible maximum" can be explored for the determination of the standard rate constant of electron transfer step k_{so} of surface CEC mechanism in the elaborated situation, following the procedure reported in Refs. [1,15].
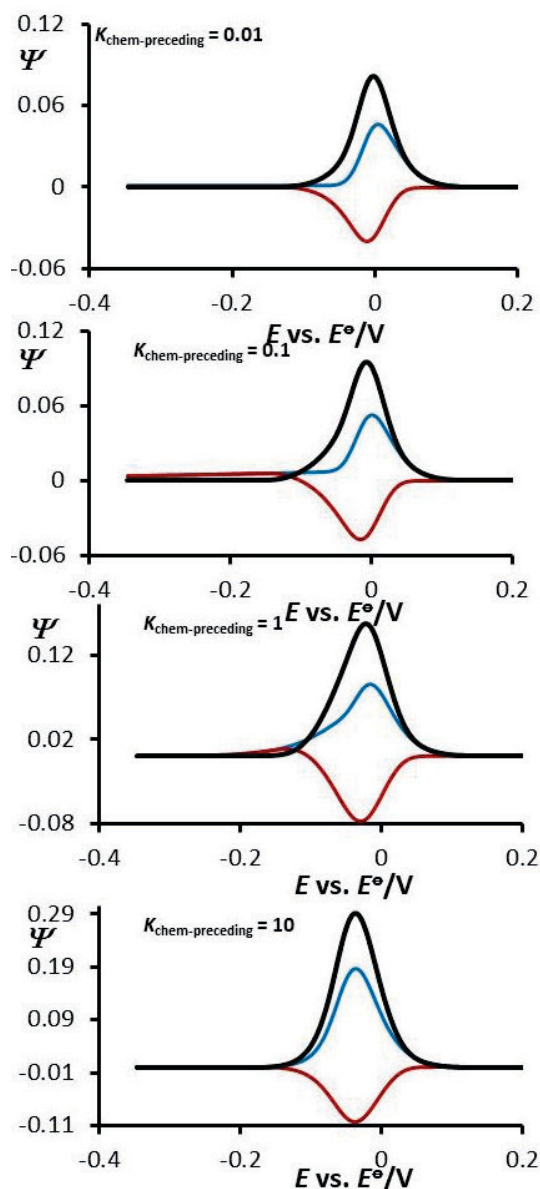

Figure 1. Theoretical SW voltammograms of a surface CEC mechanism, calculated as a function of the dimensionless rate parameter of the preceding chemical reaction $K_{chem-preceding}$. The parameters used in the simulations were: SW amplitude E_{SW} = 50 mV, step of the potential SW pulses dE = 4 mV, temperature T = 298 K, SW frequency f = 10 Hz. In all calculations, the electron transfer coefficient was set to α = 0.5, while the number of electrons exchanged was n = 2. The magnitude of dimensionless parameter related to the electron transfer step of electrode reaction was set to K_{ET} = 0.2. The equilibrium constant of the preceding chemical step was $K_{eq,\ preceding}$ = 0.1. The parameters of the follow up chemical step were set to: $K_{eq,\ follow\ up}$ = 0.001; and $K_{chem-follow\ up}$ = 0.001. The values of $K_{chem-preceding}$ are given in the charts.
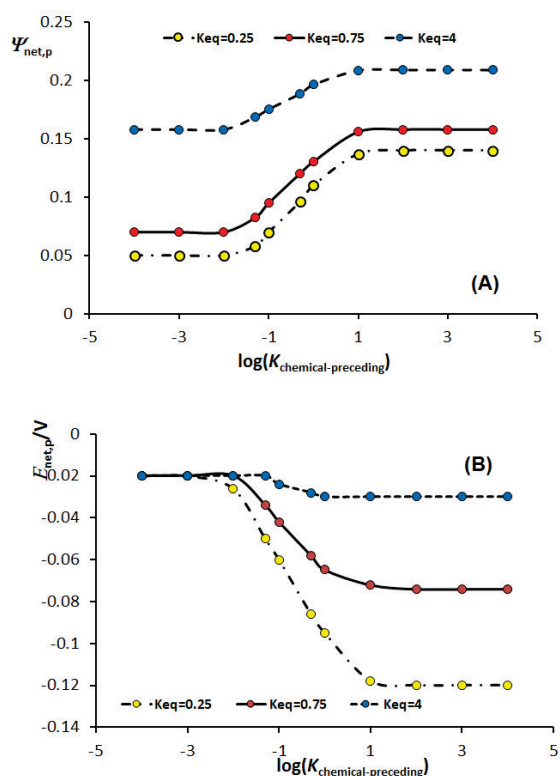
Figure 3. "Qusireversible maxima" of surface CEC mechanism recorded as a function of the magnitude of the dimensionless chemical rate parameter of preceding chemical reaction $K_{chem-preceding}$. The magnitude of the equilibrium constant of preceding chemical reaction was set to: $K_{eq, preceding} = 0.5$, while the magnitudes of $K_{chem-preceding}$ were set to: 0.1 (1); 1 (2); 10 (3) and 100 (4). Other simulation parameters were same as those in Figure 1.

Figure 2. Effect of the rate of the preceding chemical step (expressed via $\log(K_{chem-preceding})$ to the net peak currents $\Psi_{net,p}$(A) and net peak potentials $E_{net,p}$(B) of SW voltammograms of surface CEC mechanism. The magnitude of $K_{ET} = 0.1$, while the magnitudes of the equilibrium constant of preceding chemical reactions K_{eq}, were set to: 0.25 (curve 1); 0.75 (curve 2); and 4 (curve 3) in both (A) and (B) patterns. Other simulation conditions were same as those in Figure 1.

Figure 4. "Qusireversible maxima" of surface CEC mechanism recorded as a function of the magnitude of the equilibrium constant of preceding chemical reaction $K_{eq, preceding}$. The magnitudes of the dimensionless kinetic parameter of preceding chemical reaction were set to: $K_{chem-preceding} = 0.05$, while the magnitudes of $K_{eq, preceding}$ were set to: 0.05 (1); 0.1 (2); and 1 (3). Other simulation parameters were same as those in Figure 1.

(2) If the magnitude of the equilibrium constant of preceding chemical step $K_{eq, preceding} > 10$, then the "surface EC$_{rev}$ mechanism" emerges as a limiting case of elaborated surface CEC mechanism. Since a comprehensive elaboration of a surface EC$_{rev}$ mechanism under conditions of SWV is reported in our recent work,[18] we present here just some specific features of this mechanism. A common remarkable effect of dimensionless rate parameter of follow-up chemical step $K_{chem-follow\,up}$ is shown in the simulated SW patterns at Figure 5. For values of equilibrium constant $K_{eq, follow\,up} > 10$, an increase of $K_{chem-follow\,up}$, as expected, leads to decrease of the backward SW current component. However, for moderate values of $K_{eq-follow\,up}$, an increase of the dimensionless chemical parameter in the region $-2.5 < \log(K_{chem-follow\,up}) < -1$, causes appearance of local maxima at the sigmoidal Ψ-$\log(K_{chem-follow\,up})$ curves (see Figure 6.). Even more peculiar feature in Figure 6. (in region $-2 \leq \log(K_{eq, follow\,up}) \leq 1$), is that peak current of re-oxidation process (which should commonly decrease by
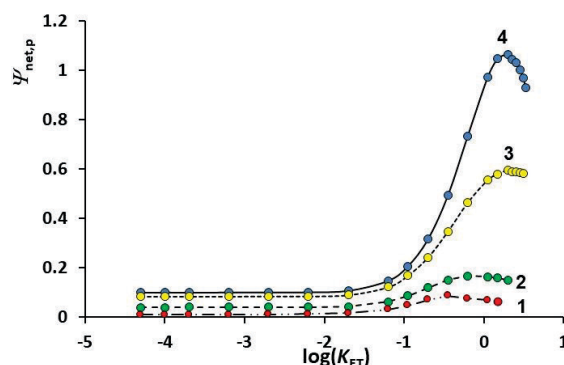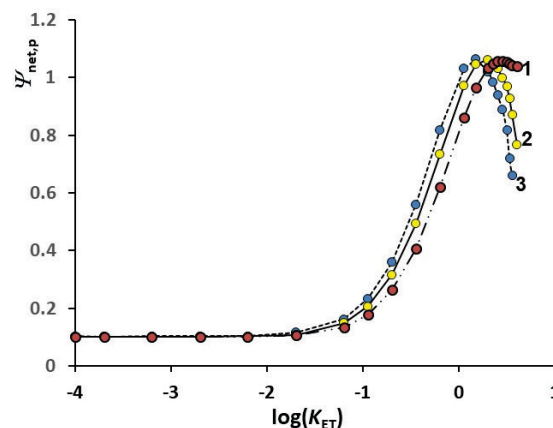
an increase of $K_{chem-follow\,up}$) gains in intensity, as chemical rate parameter gets higher values in the region $-2.5 < \log(K_{chem-follow\,up}) < -1$.

Some of the origins of this phenomenon of surface EC$_{rev}$ mechanism in SWV are elaborated in Refs. [16,18]. Shortly, the interplay of specific chronoamperometric features of this mechanism, combined with the chemical and redox transformations that take place in the so-called
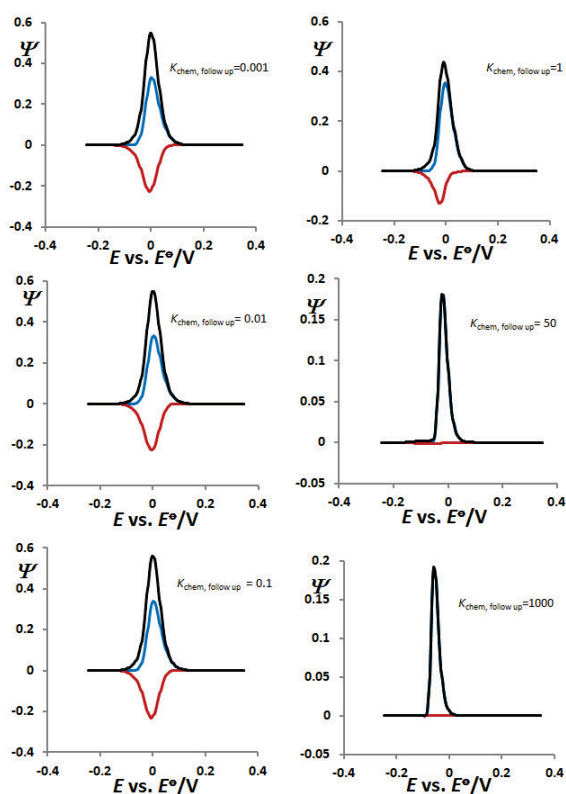
Figure 5. Theoretical SW voltammograms of a surface CEC mechanism, calculated as a function of the dimensionless rate parameter of the follow up chemical reaction $K_{chem-followup}$. The equilibrium constant of the preceding chemical step was $K_{eq, preceding} = 10$, while the value of dimensionless rate parameter of preceding chemical reaction was $K_{chem-preceding} = 100$. The values of $K_{chem-follow up}$ are given in the charts. Other simulation conditions were same as those in Figure 1.

Figure 6. Ratio of the |oxidation *vs.* reduction| peak currents of the SW voltammograms of surface CEC mechanism as a function of the logarithm of the dimensionless chemical rate parameter of follow up chemical reaction-log($K_{chem-follow up}$).[18] The magnitudes of the equilibrium constant of follow up chemical reaction were set to: $K_{eq, follow up} = 0.1$ (1); 1 (2) and 10 (3). Other simulation parameters were same as those in Figure 5.

Figure 7. "Qusireversible maxima" of surface CEC mechanism recorded as a function of the magnitude of the dimensionless chemical rate parameter of follow up chemical reaction $K_{chem-follow up}$. The magnitude of the equilibrium constant of follow up chemical reaction was set to: $K_{eq, follow up} = 0.5$, while the magnitudes of $K_{chem-follow up}$ were set to 0.0125 (1); 0.0275 (2); 0.0525 (3) and 0.0775 (4).[18] Other simulation parameters were same as those in Figure 5.

"dead time" (or non-current measuring time segment) of potential SW pulses, leads to the appearance of local maxima observed at sigmoidal curves in Figure 6. Another important aspect to be noticed in surface EC_{rev} mechanism is the dependence of the position of "quasireversible maximum" as a function of $K_{chem-follow up}$ (Figure 7.), which appears in region of moderate values of $K_{eq, follow up}$.[18] Roughly, in the regions of $-2 \leq \log(K_{eq, follow up}) \leq 0$, an increase of the rate of chemical step in region $-2 \leq \log(K_{chem-follow up}) \leq -0.3$, is followed by a shift of the position of the "quasireversible maximum" towards higher values of K_{ET}. This finding implies that the rate of the follow up chemical reaction might influence the apparent rate of electron transfer step of surface EC_{rev} mechanism. Following the procedure elaborated in Ref. [18], it is possible to evaluate all relevant kinetic and thermodynamic parameters related to the chemical and electron transfer step of given surface EC_{rev} mechanism.
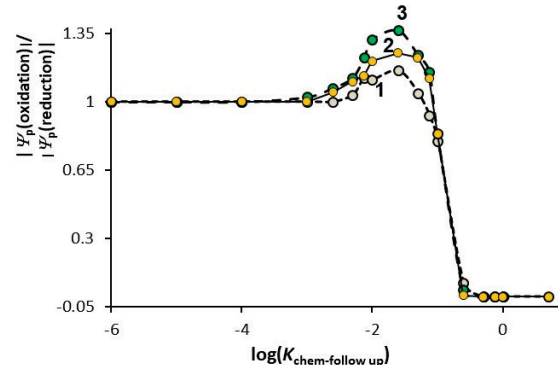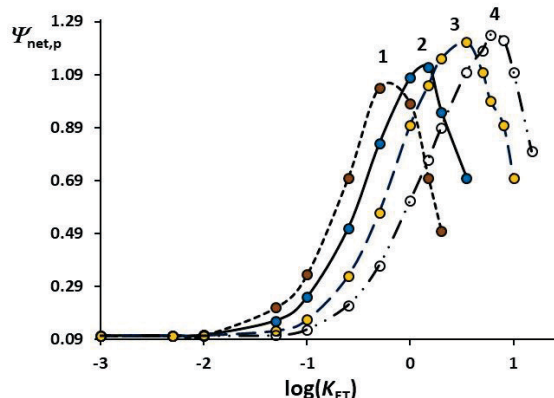
A remarkable feature of all surface electrode mechanisms is the "splitting" of the net SW voltammetric peaks.[1,31] This phenomenon can be achieved under the influence of the kinetics of electron transfer step, and by increasing the magnitude of SW amplitude.[1] In Refs. [1,31], an elegant approach is elaborated to access the kinetics of electrode reaction, by exploring the features of "splitting of net SW peaks". When the electron transfer is fast, then the electrochemical conversion of Ox(ads) to Red(ads) will take

place in a very small time-segment at the beginning of potential SW pulses. Consequently, in time period in which current is measured at the end of potential SW pulses, only a small amounts of Ox(ads) (or Red) will remain available for transformation at the working electrode. This will cause small currents to be detected in SWV experiments of surface reactions featuring fast rate of electron transfer step.[1,31] Moreover, at higher kinetics of electrode reaction, there is a shift of reduction process towards more positive potentials, and of the oxidation process towards more negative potentials. A consequence of this sequence of events is splitting of the net SWV response to two peaks. The splitting of net SW peak phenomenon is reported to be a useful methodology for estimation of standard rate constant of electron transfer k_{so} as elaborated in Refs. [1,31]. Some relevant features of "splitting phenomena of SW voltammetric peaks" for surface $C_{rev}E$ and surface EC_{rev} mechanism are elaborated in Ref. [15] and in Ref. [18], respectively. Shown in Figures 8. and 9. is the splitting feature, simulated in a set of SW voltammograms of surface $C_{rev}E$ and surface EC_{rev} systems, correspondingly. Voltammograms are calculated as a function of the corresponding dimensionless chemical rate parameters by both mechanisms.

Although the effect of K_{chem} at the voltammograms in Figures 8. and 9. appears very similar, one observes crucial differences that distinguish both mechanisms. At surface $C_{rev}E$ mechanisam, an initial increase of $K_{chem-preceding}$ from 0.00001 to 0.03 leads to disappearance of the splitting phenomenon (Figure 8.a–b), which eventually reappears at higher values of $K_{chem-preceding}$ (Figure 8.c–d). This is not the case for the splitting phenomenon at surface EC_{rev} mechanism, where an increase of $K_{chem-follow up}$ above 0.001 causes initial (more intensive) increase of the backward (re-oxidation) SWV current component (Figure 9.a–b). Additional increase of dimensionless rate parameter related to follow up chemical reaction leads to a permanent disappearance of the splitting phenomenon of net peak, and only a single SW peak exists observed by further increase of $K_{chem-follow up}$ (Figure 9.c–d). The patterns presented in Figures 8. and 9. can be explored as simple diagnostic criteria to distinguish between the surface $C_{rev}E$ and the surface EC_{rev} mechanisms, in situation of fast kinetics of electron exchange process between the working electrode and the Ox/Red couple.

(3) If both equilibrium constants of the chemical steps of surface CEC mechanism feature moderate-to-low values, i.e. $\log(K_{eq, preceding}) \leq 0$, and $\log(K_{eq, follow up}) \leq 0$, then one observes very complex voltammetric patterns of this system. In such scenario, alongside to their dependence on the kinetics of electron transfer step, the shape and the position of calculated voltammetric outputs is complex function of the kinetics and thermodynamics of both
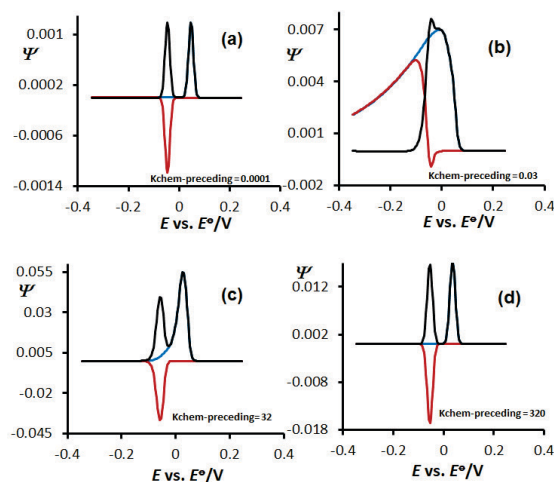

Figure 8. Theoretical SW voltammograms of surface $C_{rev}E$ mechanism featuring fast electrode reaction ($K_{ET} = 2$), calculated as a function of the dimensionless rate parameter of the preceding chemical reaction $K_{chem-preceding}$. The equilibrium constant of the preceding chemical reaction was set to $K_{eq, preceding} = 10$. The values of $K_{chem-preceding}$ are given in the charts. Other simulation conditions are same as those in Figure 1.
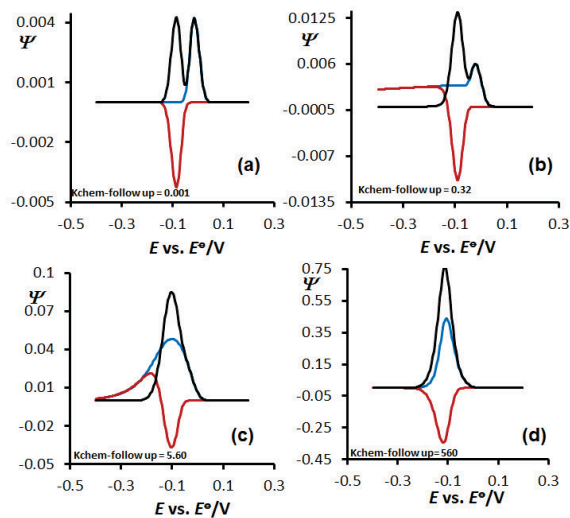

Figure 9. Theoretical SW voltammograms of surface EC_{rev} mechanism featuring fast electrode reaction ($K_{ET} = 1.25$), calculated as a function of the dimensionless rate parameter of the follow up chemical reaction $K_{chem-follow up}$. The equilibrium constant of the follow up chemical reaction was set to $K_{eq, follow up} = 10$. The values of $K_{chem-follow up}$ are given in the charts. Other simulation conditions are same as those in Figure 1.

chemical steps. The entire complexity, however, should be even more expressed in real experiments. This comes out from the fact that the SW frequency affects simultaneously

all kinetic parameters, i.e. $K_{chem-preceding}$, $K_{chem-follow\ up}$, and K_{ET}. Although the SW frequency affects all rate parameters in a same way, yet all of them ($K_{chem-preceding}$, $K_{chem-follow\ up}$, and K_{ET}) exhibit quite different influence to the features of calculated SW voltammograms. In general, for an overall reductive mechanism, a decrease of K_{ET} causes a shift of the net SWV peak potentials to more negative values. While an increase of the dimensionless rate parameter of preceding chemical reaction $K_{chem-preceding}$ leads to shifting of the net SWV peak potentials to more negative values,[15] opposite holds true for the dimensionless rate parameter of follow up chemical step $K_{chem-follow\ up}$.[18] In addition, all three dimensionless rate parameters exhibit rather complex influence to the current components of simulated SW voltammograms, as reported in Refs. [1,6,7,15,18]. Since many methods developed to access relevant kinetic parameters in SWV rely on frequency (or time) analysis,[1–4,12–13] such a survey applied to a surface CEC mechanism is supposed to generate complex voltammetric scenarios, when both $\log(K_{eq,\ preceding}) \leq 0$, and $\log(K_{eq,\ follow\ up}) \leq 0$. However, the SW frequency analysis can reveal important aspects about recognizing the surface CEC mechanism, and can help in designing proper experiments for getting access to all relevant parameters affecting this complex system. Two examples of a theoretical SW frequency analysis in surface CEC mechanism are shown in Figures 10. and 11. SW voltammograms are simulated at equal equilibrium constants of both chemical steps i.e. $K_{eq,\ preceding} = K_{eq,\ follow\ up} = 0.1$, and magnitudes of rate parameters of chemical steps $\varepsilon = 1\ s^{-1}$ and $z = 0.1\ s^{-1}$ (for the preceding and the follow up chemical steps, correspondingly). Voltammograms in Figure 10. are calculated for a value of the standard rate constant of electron transfer of $k_s^{\oplus} = 1\ s^{-1}$, while $k_s^{\oplus} = 100\ s^{-1}$ was set for the voltammograms in Figure 11. As the SW frequency gets values between 0.01 Hz and 1 Hz (Figure 10.a–c), one observes that the kinetics of preceding chemical step has a dominant effect. This is obvious from the features of all current components of simulated SW voltammetric patterns that resemble to those of a surface $C_{rev}E$ mechanism. In addition, in this region of SW frequencies, the net SW peak potential shifts to more positive potentials by increasing f, a feature typical for surface $C_{rev}E$ systems.[1,15] However, as the SW frequency is higher than 1 Hz, then the kinetics of the follow up chemical step starts to have major effect, which is visible via the diminishment of the backward current component,[18] as expected for a surface EC_{rev} mechanism (Figure 10.d). Finally, for SW frequencies larger than 20 Hz (Figure 10.e–f), the slow kinetics of the electron transfer step (small K_{ET}) controls the overall kinetics of the surface CEC mechanism, resulting with low currents measured. The voltammograms in Figure 10. imply that in a relatively small range of SW frequencies, roughly between 1 Hz and 30 Hz, one detects

three different kinetics exhibiting the dominating effect to the simulated voltammograms. Even more complex voltammetric patterns exist at surface CEC systems in which the electron transfer steps feature large values of $k_s^{\oplus}$ (Figure 11.). Although rate constant of electron transfer is rather high, which should result in splitting of the net SW voltammogram at small frequencies, this is not the case at Figure 11.a–d. Again, for small frequencies in region between 0.01 Hz and 10 Hz, the kinetics of preceding chemical step is major rate parameter that controls the features of simulated voltammograms. Only in a small frequency region between 20 Hz and 50 Hz one observes the splitting of the net SWV peaks (Figure 11.e). The splitting phenomenon vanishes at frequencies larger than 50 Hz, and the voltammetric patterns get shape in which the kinetics of electron transfer step dictates mainly the
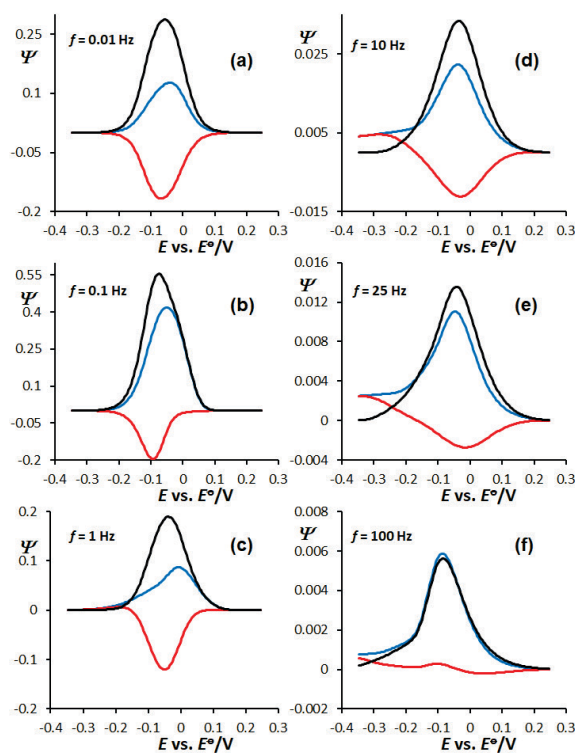

Figure 10. Theoretical SW voltammograms of a surface CEC mechanism, calculated as a function of the SW frequency. Voltammograms are calculated by assuming equal magnitudes of both equilibrium constants, i.e. $K_{eq,\ preceding} = K_{eq,\ follow\ up} = 0.1$, and for values of rate parameters of the preceding and follow up chemical steps of $\varepsilon = 1\ s^{-1}$, and $z = 0.1\ s^{-1}$, correspondingly. The standard rate constant of electron transfer was set to $k_s^{\oplus} = 1\ s^{-1}$. The magnitudes of the SW frequencies applied are given in the charts. SW amplitude was set to $E_{SW} = 60$ mV, while other simulations parameters were same as those in Figure 1.
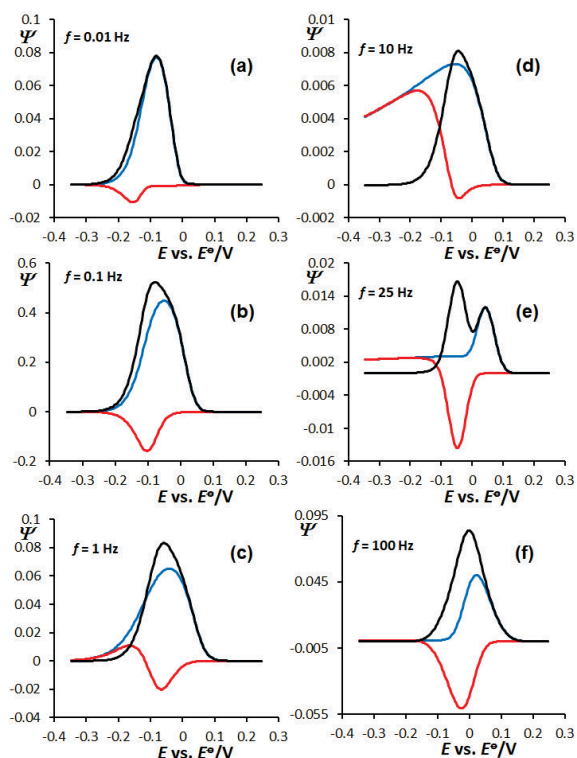
Figure 11. Theoretical SW voltammograms of a surface CEC mechanism, calculated as a function of the SW frequency. Voltammograms are calculated by assuming equal magnitudes of both equilibrium constants, i.e. $K_{eq, preceding}$ = $K_{eq, follow up}$ = 0.1, and for values of rate parameters of the preceding and follow up chemical steps of ε = 1 s^{-1}, and z = 0.1 s^{-1}, correspondingly. The standard rate constant of electron transfer was set to $\boldsymbol{k_s^{\circ} = 100\,s^{-1}}$. The magnitudes of the SW frequencies applied are given in the charts. SW amplitude was set to E_{SW} = 60 mV, while other simulation parameters were same as those in Figure 1.

voltammetric characteristics (Figure 11.f). The voltammograms in Figures 10. and 11. imply that the frequency analysis, although showing a very complex effect, can help in recognizing the surface CEC mechanism. This is because this parameter will produce rather specific SWV patterns in relatively small range of applied frequencies. This information, as explained in the next section, might help to design proper experiments for the determination of most of the relevant kinetic parameters affecting this complex mechanism.

CONCLUSIONS

Although there are important chemical systems undergoing electrode transformation according to a surface CEC mechanism, there is a need of theoretical studies of this mechanism under conditions of square-wave voltammetry.

In this work we present a set of relevant results of a surface CEC mechanism, in which we mainly elaborate the effect of rate parameters of both, the preceding and the follow up chemical steps to the features of calculated SW voltammograms. Since the interplay of all kinetic and thermodynamic parameters involved in this mechanism might result in very complex voltammetric patterns, we tried to simplify the surface CEC mechanism to two limiting simpler mechanisms. If the equilibrium constant of preceding chemical step is $\log(K_{eq,\ preceding})$ > 1, then the entire surface CEC mechanism can be approximated with a surface EC$_{rev}$ mechanism. If $\log(K_{eq,\ follow\ up})$ ≤ −2.3, and for small values of chemical rate parameter of follow up step, then the entire mechanism can be described with the relevant features of a surface C$_{rev}$E mechanism. However, if both $\log(K_{eq,\ preceding})$ ≤ 0, and $\log(K_{eq,\ follow\ up})$ ≤ 0, then one witnesses a complex voltammetric interplay of all thermodynamic and kinetic parameters involved in this mechanism. In such scenario, it is of crucial interest to establish criteria first to recognize, and afterwards to simplify (if possible) the surface CEC mechanism to one of its limiting cases. Such an approach will enable to explore the methodologies reported for surface C$_{rev}$E[15] and surface EC$_{rev}$ mechanism[18] to get access to all relevant physical parameters. The first indicator of occurrence of a surface CEC mechanism might come from a SW frequency analysis. Such an analysis can generate SW voltammograms that can change its characteristics in a certain (narrow) region of applied frequencies (see Figures 10.c–e and 11.c–e). Once the surface CEC mechanism is recognized, the second experimental step is to simplify it to a surface C$_{rev}$E mechanism. This can be done in voltammetric experiments performed at constant frequency, and by decreasing the kinetics of follow up chemical step by modifying the molar concentration of substrate "Y" in electrochemical cell.[18] Once the surface CEC mechanism is turned to a simple surface C$_{rev}$E system, then one can explore the methods reported in Ref. [15] to get access to kinetic and thermodynamic parameters relevant to this mechanism. In the next step, also by modifying (increasing) the molar concentration of substrate "Y", one can explore the feature of shifting of "quasireversible maximum" as a function of concentration of substrate "Y" (Figure 7.) as a mean to get access to the kinetic parameter of the follow up chemical step.[18] The feature presented in Figure 7. is specific only for surface EC$_{rev}$ mechanism,[18] since the kinetics of preceding chemical step does not affect the "quasireversible maximum" as elaborated in Ref. [15]. For the determination of the electron transfer coefficient α, one can take advantage of the SWV methodology reported in Ref. [32]. It is worth mentioning that due to rather complex outputs of this mechanism, one has to take into consideration many specific features of simpler surface CE and surface EC

systems that are extensively elaborated from our groups under conditions of SWV in Ref. [15] and Ref. [18], correspondingly. Readers are also advised to the supplementary MATHCAD file provided in this work, which might serve as a useful playground for performing other valuable simulations on this complex mechanism.

Acknowledgment. All authors thank the "Goce Delcev" University in Stip, Macedonia for the support.

Supplementary Information. Supporting information to the paper is attached to the electronic version of the article at: https://doi.org/10.5562/cca3768.

PDF files with attached documents are best viewed with Adobe Acrobat Reader which is free and can be downloaded from Adobe's web site.

REFERENCES

[1] V. Mirčeski, Š. Komorsky-Lovrić, M. Lovrić, *Square-wave voltammetry.Theory and application* (F. Scholz, ed.), Springer, Berlin, Germany, **2007**. https://doi.org/10.1007/978-3-540-73740-7

[2] R. G. Compton, C. E. Banks, *Understanding voltammetry*, 2nd edition, ImperialCollege Press, London, UK, **2011**.

[3] A. J. Bard, L. R. Faulkner, *Electrochemical methods. Fundamentals andapplications,* 3rd edition, John Wiley & Sons, Inc., **2004**.

[4] A. Molina, J. Gonzales*, Pulse voltammetry in physical electrochemistry and electroanalysis*, in *Monographs in electrochemistry* (F. Scholz, ed.), Berlin, Heidelberg, Springer, **2016**. https://doi.org/10.1007/978-3-319-21251-7_4

[5] R. Gulaboski, V. Mirceski, *Maced. J. Chem. Chem. Eng.* **2020**, *39*, 153–166. https://doi.org/10.20450/mjcce.2020.2152

[6] R. Gulaboski, V. Mirčeski, I. Bogeski, *J. Solid State Electrochem.* **2012**, *16*, 2315–2328. https://doi.org/10.1007/s10008-011-1397-5

[7] V. Mirceski, R. Gulaboski, M. Lovric, I. Bogeski, R. Kappl, M. Hoth, *Electroanalysis* **2013**, *25*, 2411–2422. https://doi.org/10.1002/elan.201300369

[8] V. Mirceski, R. Gulaboski, *Maced. J. Chem. Chem. Eng*. **2014**, *33*, 1–12.

[9] P. N. Barlett, *Bioelectrochemistry-Fundamentals, experimental techniques andapplication*, Wiley, Chichester, **2008**.

[10] M. Saveant, Elements of molecular and biomolecular electrochemistry: Anelectrochemical approach to electron transfer chemistry, Hoboken, NJ, Wiley, **2006**. https://doi.org/10.1002/0471758078

[11] R. Gulaboski, V. Mirceski, M. Lovric, *J. Solid State Electrochem.* **2019**, *23*, 2493–2506. https://doi.org/10.1007/s10008-019-04320-7

[12] F. A. Armstrong, *Voltammetry of proteins* In: *Encyclopaedia ofelectrochemistry* (A. J. Bard, M. Stratmann, G. S. Wilson (eds.)), vol. 9, WileyVCH, Weinheim, **2002**. https://doi.org/10.1002/9783527610426.bard090001

[13] C. Leger, P. Bertrand, *Chem. Rev*. **2007**, *108*, 2379–2438. https://doi.org/10.1021/cr0680742

[14] P. Kokoskarova, R. Gulaboski, *Electroanalysis* **2020**, *32*, 333–344. https://doi.org/10.1002/elan.201900491

[15] R. Gulaboski, V. Mirceski, M. Lovric, I. Bogeski, *Electrochem. Commun*. **2005**, *7*, 515–522. https://doi.org/10.1016/j.elecom.2005.03.009

[16] R. Gulaboski, *Electroanalysis* **2019**, *31*, 545–533. https://doi.org/10.1002/elan.201800739

[17] R. Gulaboski, *J. Solid State Electrochem*. **2009**, *13*, 1015–1024. https://doi.org/10.1007/s10008-008-0665-5

[18] R. Gulaboski, M. Janeva, V. Maksimova, *Electroanalysis* **2019**, *31*, 946–956. https://doi.org/10.1002/elan.201900028

[19] R. Gulaboski, P. Kokoskarova, S. Petkovska, *Croat. Chem. Acta* **2018**, *91*, 377–382. https://doi.org/10.5562/cca3383

[20] R. Gulaboski, P. Kokoskarova, S. Risafova, *J. Electroanal. Chem*. **2020**, *868*, 114189. https://doi.org/10.1016/j.jelechem.2020.114189

[21] R. Gulaboski, V. Mirceski, *Electrochim. Acta*, **2015**, *167*, 219–225. https://doi.org/10.1016/j.electacta.2015.03.175

[22] M. Lopez-Tenes, E. Laborda, A. Molina, R. G. Compton, *Anal. Chem*. **2019**, *91*, 6072–6079. https://doi.org/10.1021/acs.analchem.9b00616

[23] M. Rafiee, D. Nematollahi, H. Salehzadeh, *Electrochim. Acta* **2011**, *56*, 9946–9952. https://doi.org/10.1016/j.electacta.2011.08.083

[24] O. Nekrassova, N. S. Lawrence, R. G. Compton, *Electroanalysis* **2003**, *15*, 1501–1505. https://doi.org/10.1002/elan.200302766

[25] H. Salehzadeh, D. Nematollahi, *Electrochim. Acta* **2013**, *111*, 909–915. https://doi.org/10.1016/j.electacta.2013.08.093

[26] M. T. Carter, M. Rodriguez, A. J. Bard, *J. Am. Chem. Soc*. **1989**, *111*, 8901–8911. https://doi.org/10.1021/ja00206a020

[27] V. Pierroz, T. Joshi, A. Leonidova, C. Mari, J. Schur, I. Ott, L. Spiccia, S.Ferrari, G. Gasser, *J. Am. Chem Soc*. **2012**, *134*, 20376–20387. https://doi.org/10.1021/ja307288s

[28] Ch. Batchelor-McAuley, Q. Li, S. M. Dapin, R. G. Compton, *J. Phys. Chem. B* **2010**, 114, 4094–4100. https://doi.org/10.1021/jp1008187

[29] A. De Rache, T. Doneux, C. Buess-Herman, *Anal. Chem.* **2014**, *86*, 8057–8065.
https://doi.org/10.1021/ac500791s

[30] J. A. Ribeiro, C. M. Pereira, F. Silva, *Electrochim. Acta* **2015**, *180*, 687–694.
https://doi.org/10.1016/j.electacta.2015.08.074

[31] V. Mirceski, M. Lovric, *Electroanalysis* **1997**, *9*, 1283–1287.
https://doi.org/10.1002/elan.1140091613

[32] R. Gulaboski, M. Lovric, V. Mirceski, I. Bogeski, M. Hoth, *Biophys. Chem.* **2008**, *138*, 130–137.
https://doi.org/10.1016/j.bpc.2008.09.015